The FreqTag toolbox: A principled approach to analyzing electrophysiological time series in frequency tagging paradigms

Jessica Sanches Braga Figueira[1], Ethan Kutlu[2], Lisa S. Scott[2], & Andreas Keil[1]

[1]Center for the Study of Emotion and Attention, University of Florida, Gainesville, FL, United States of America

[2]Department of Psychology, University of Florida, Gainesville, FL, USA

Corresponding Author: Jessica Sanches Braga Figueira

jessica.sanchesb@ufl.edu

Center for Study of Emotion and Attention

University of Florida

+1 (352) 392-2439

3063 Long Leaf Rd, Gainesville, FL 32608

ABSTRACT

Steady-state visual evoked potential (ssVEP) frequency tagging is an increasingly used method in electrophysiological studies of visual attention and perception. Frequency tagging is suitable for studies examining a wide range of populations, including infants and children. Frequency tagging involves the presentation of different elements of a visual array at different temporal rates, thus using stimulus timing to "tag" the brain response to a given element by means of a unique time signature. Leveraging the strength of the ssVEP frequency tagging method to isolate brain responses to concurrently presented and spatially overlapping visual objects requires specific signal processing methods. Here, we introduce the FreqTag suite of functions, an open source MATLAB toolbox. The purpose of the FreqTag toolbox is three-fold. First, it will equip users with a set of transparent and reproducible analytical tools for the analysis of ssVEP data. Second, the toolbox is designed to illustrate fundamental features of frequency domain and time-frequency domain approaches. Finally, decision criteria for the application of different functions and analyses are described. To promote reproducibility, raw algorithms are provided in a modular fashion, without additional hidden functions or transformations. This approach is intended to facilitate a fundamental understanding of the transformations and algorithmic steps in FreqTag, and to allow users to visualize and test each step in the toolbox.

***Keywords**:* steady-state visual evoked potential (ssVEP); frequency tagging; frequency domain; time-frequency domain; MATLAB; FreqTag

1-Introduction

The electroencephalogram (EEG) relies on the non-invasive recording of brain electric activity through sensors that are placed on the scalp to provide a rich source of information about ongoing brain activity at a millisecond scale (Jackson & Bolger, 2014; Nunez et al., 2006). EEG signals have been used to study a wide range of neural processes, including spectral properties of resting EEG (Donoghue et al., 2020; Rogala et al., 2020), task-driven studies measuring event-related potentials (ERP, for review see: Luck & Kappenman, 2013; Handy, 2004; Woodman, 2013) and steady-state visual evoked potentials (ssVEPs, for review see: Norcia et al., 2015; Vialatte et al., 2010). EEG methods are also extensively used in developmental populations from early infancy through adolescence (for review see: Barry-Anwar et al., 2020; Bell & Cuevas, 2012; Riggins & Scott, 2020). The present report focuses on one specific EEG-based method: frequency-tagging with steady-state visual evoked potentials (Norcia et al., 2015; Wieser et al., 2016). Studies measuring ssVEPs in adults have substantially contributed to our understanding of visual processes including selective attention, figure-ground segregation, and adaptation (for review see Norcia et al., 2015).

The ssVEP is a neurophysiological response to a periodic visual stimulus. It is evoked by stimuli that are periodically modulated in luminance (i.e., flickered) or contrast (e.g., pattern-reversed) typically at temporal rates above 3 Hz (Odom et al., 2004). Both the luminance-evoked and contrast-evoked ssVEP possess high signal-to-noise ratio and are robust to noisy recording conditions, allowing researchers flexibility regarding dimensions of interest within stimuli (Appelbaum et al., 2006; Keil, 2013). Luminance-evoked ssVEPs reflect visuocortical activation based on input across the retina, whereas contrast-evoked ssVEPs at constant luminance tend to emphasize foveal inputs which are more circumscribed in the visual cortex (Di Russo et al., 2006).

Because they are defined by their temporal frequency, ssVEPs may be extracted from scalp-recorded EEG signals in the frequency domain, by calculating the amplitude spectrum of the EEG segments of interest.

The ssVEP response typically consists of robust oscillatory activity at the exact modulation frequency—driving frequency—as well as at its higher harmonics (integer multiples of the driving frequency). Thus, an LED light flickering at 12 Hz evokes ssVEPs at 12 Hz, but may also prompt responses at 24 Hz, 36 Hz, etc., depending on the composition of the stimulus array and the extent to which the visual response is linear or non-linear (Norcia et al., 2015). Source estimation of scalp-recorded ssVEPs (Di Russo et al., 2006) as well as combined ssVEP-fMRI work (Petro et al., 2017) have converged to show that ssVEPs appear to be generated primarily in the striate cortex (V1) with contributions from extrastriate regions (for review see; Vialatte et al., 2010).

One key feature of the ssVEP outlined in the present report is its use in frequency tagging. This technique enables researchers to independently quantify the visuocortical response to multiple stimuli, even when these stimuli are presented at the same time and at overlapping screen locations (Tononi et al., 1998; Wang et al., 2007; Zhigalov et al., 2019). Thus, complex stimulus arrays may be used and a unique visuocortical response to each element of the complex array is evoked by periodically modulating each element at a different frequency. Frequency domain (spectral) analyses can then be used to independently quantify the response of each stimulus in the amplitude spectrum of the EEG data. For example, frequency tagging has been previously used for quantifying neural competition between concurrent visuocortical representations evoked by simultaneously present and overlapping stimuli (Appelbaum et al., 2006; Bach & Meigen, 1992), which is difficult to accomplish with other neuroscience methods.

In developmental samples, ssVEPs have been used to assess lower-level sensory processes in infants (Braddick et al., 1986; Gilmore et al., 2007; Hamer & Norcia, 1994), but also to investigate higher cognitive processes such as overt and covert visual attention (Christodoulou et al., 2018; Robertson et al., 2012), contour integration (Baker et al., 2011), face or object processing (Barry-Anwar et al., 2018; Buiatti et al., 2019; de Heering & Rossion, 2015; Farzin et al., 2012; Leleu et al., 2014; Lochy et al., 2019; Peykarjou et al., 2017; Vettori et al., 2020), number sense (Park, 2018), and event processing (Köster et al., 2019). Studying development using recordings of ssVEPs are particularly useful relative to other EEG measures for a variety of reasons. First, infant and child EEG data often include an increased amount of noise relative to adults. Because ssVEP analyses focus on a narrow set of frequency bands, the signal to noise ratio is very high because only the noise present in the driving frequency bins is relevant (Regan, 1989). Second, the amount of time required to collect high quality ssVEP responses from infants is less than what is typically needed for ERPs. Furthermore, several conditions or tasks can be combined in a single session, reducing attrition and increasing statistical power. The shorter session duration requirement for ssVEP tasks compared to other EEG tasks is also important because it is often difficult for infants to complete tasks that take longer than about 15 minutes (including breaks).

Studies using frequency tagging of multiple stimuli highlight the promise of using this technique for studying cognitive and perceptual development (Baker et al., 2011; Buiatti et al., 2019; Vettori et al., 2020). The present report demonstrates key analytical procedures for analyzing frequency tagging data for both developmental and adult samples. The report is accompanied by example adult and infant data and a MATLAB toolbox (FreqTag, https://github.com/csea-lab/freqTag) containing algorithms for performing analyses on frequency tagged data. Several methodological details not covered in this paper are explained in the documentation accompanying

the toolbox. Many existing EEG analysis tools may be used for the same purpose (e.g., see Mouraux & Iannetti, 2008 - Letswave, RRID:SCR_016414). The aim of the present toolbox is to illustrate core analytical principles using barebones algorithms, with the intention to promote a deeper understanding of the method and increase user confidence. Specifically, this report illustrates spectral analysis based on discrete Fourier transform, and analysis in the time-frequency domain, where the neural time course at each tagging frequency is individually extracted using the Hilbert transformation. We also demonstrate the use of the sliding window averaging technique, suitable for studies with fewer trials, as is sometimes the case for developmental EEG work. The code (https://github.com/csea-lab/freqTag) and example datasets (https://osf.io/e5vuf/) are publicly available.

2-Methods and Materials

2.1- Hardware and software needed to implement a frequency tagging protocol

As discussed above, many different research questions may be pursued using frequency tagging. Thus, many different types of stimuli may be used, including stimuli in multiple modalities (Giabbiconi et al., 2016; Riels et al., 2021). Regardless of the stimulus type and modality used, it is crucial that researchers ensure accurate timing of each stimulus. For visual stimuli, the tagging frequencies available are primarily determined by the display device used. The refresh rate denotes the frequency (in Hz) at which the display can update its content. Not all visual displays are suitable for evoking ssVEPs, and some of the key properties needed for regular, accurate, periodic stimulation are more likely to be found in Cathode-ray tube (CRT) monitors, compared to light-emitting diode displays (LED), and liquid crystal displays (LCD), since both LCD and LED may present (a) response delays caused by digital processing time as well as (b)

temporal smearing due to slow and non-symmetric black to white and white to black response times, especially at high stimulation rates. Several companies offer non-CRT solutions that provide high refresh rates and rapid transition times from black to white and vice versa.

Successful implementations of tagging protocols are also accomplished with hardware solutions where custom circuit boards drive individual light-emitting diodes controlled by a microcomputer (e.g., Gulbinaite et al., 2019). A comprehensive discussion of display systems is outside the scope of this report, and readers are referred to the extant discussions in the literature (e.g., Wang & Nikolic, 2011). Likewise, graphic processing demands are high when using frequency tagging, and researchers should consider state-of-the art graphics cards rather than on-board graphics, which are often insufficient for ensuring accurate ssVEP stimulation.

Not all software used to generate and control visual stimuli in the cognitive neuroscience laboratory is suitable for use with ssVEP frequency tagging given that the technique exerts high demands regarding graphic card control and timing accuracy (Jaganathan et al., 2005). It is therefore highly recommended to test and validate the intended timing before beginning data collection. Light sensitive diodes and similar devices are readily available to capture and store luminance changes directly from the display device, allowing researchers to examine the overlap between the control software's specifications and the reality on the display. Suitable software packages for experimental control include psychtoolbox, psychopy, and presentation, in addition to low-level code written in various programming languages. We provide example code written in Psychtoolbox (taggingdemo.m) together with the FreqTaq toolbox.

2.2-Implementing the stimulus array

There are several parameters to be considered when using frequency tagging tasks such as the monitor refresh rate, the duration of the stimulus presentation within each trial, and the EEG

sampling rate. When using on-off flicker, the frequencies available for tagging on a 60 Hz monitor are at the ratio of 60 and the integers from 2 to 20, i.e., at 60/2, 60/3, 60/4, … 60/20, resulting in potential frequencies at 30, 20, 15, 12, 10, 8.571, 7.5, 6.667, 6.0, 5.455, 5.0, 4.615, 4.286, 4.0, 3.75, 3.529, 3.333, 3.158, and 3.0 Hz. This is equivalent to determining the tagging frequencies based on the wavelength of the refresh rate, also known as the refresh interval, which in the case of the 60 Hz monitor is 1000/60 = 16.66ms. Here, the available tagging frequencies can be computed by dividing 1000 by the product of the refresh interval and the integers between 2 and 20, resulting in the same potential tagging frequencies for on-off flicker. Note that periodic presentations with other stimulation (e.g., sinusoidal, rather than on-off, modulation of luminance) may result in additional frequencies becoming available, as discussed for example by Andersen & Müller (2015).

For some applications, researchers may prefer that the two components of the ssVEP duty cycle (e.g., the on and off periods of the stimulus in a flicker-ssVEP) be of equal duration. This reduces the available tagging frequencies by 50%. In the example above, frequencies resulting from multiplying odd numbers with the refresh interval will be unavailable if on and off-periods (in luminance ssVEPs) or pattern one versus pattern two (in pattern reversal ssVEP) are to be of the same duration. Furthermore, when using multiple frequencies for many visual objects simultaneously, researchers will want to ensure that the tagging frequencies do not exhibit harmonic relations (in which one tagging frequency is an integer multiple of another; 6 Hz and 12 Hz for example), because this prevents the independent analysis of the two spectral responses (in the example, the second harmonic of the 6 Hz stimulus is located at the fundamental driving frequency of the other stimulus, i.e., at 12 Hz).

The epoch duration, the duration of the EEG data segment used for frequency analysis, determines the spectral resolution used to quantify the ssVEP at each frequency. If the epoch is too short in duration, frequency resolution may not suffice for discriminating between the two or more frequencies used for tagging. In these cases, many researchers use padding with zeros or other suitable values, which increases the number of the bins on the x-axis of the spectrum and thus facilitates the separation of the tagging frequencies in the spectrum. It is important to note, however, that increasing the number of bins does not increase the true underlying spectral resolution because zero-padding only interpolates the information already contained in the data. It is also advisable to use epoch durations that hold integer numbers of cycles for a given tagging frequency, based on integer numbers of sample points. For example, 60 full cycles of flicker ssVEPs evoked for 6000 ms at a frequency of 10 Hz, on a 60 Hz monitor, are captured by the 6000 ms window when sampling at 500 or 1000 Hz, but not when sampling at 512 Hz. Ensuring that the data segment of interest contains integer numbers of cycles and sample points will result in frequency spectra that contain bins at the exact stimulation frequency, without additional preprocessing steps such as up-sampling and padding (for an extensive discussion of these points, see Bach & Meigen, 1999).

Planning the epoch duration and selecting the tagging frequencies such that integer cycles are available in the epoch of interest, at the sample rate used, also minimizes distortions related to so-called "spectral leaking." This term refers to the smearing of oscillatory responses across two or more bins of the spectrum, which may occur for example when there is no bin available at the exact tagging frequency. Such leaking may lead to misinterpretation of condition differences, especially when the mapping of tagging frequencies to stimuli and experimental condition is not counterbalanced across the experiment. The reader is directed to reviews and guidelines regarding

the technical aspects of ssVEP procedures (Bach & Meigen, 1999; Keil et al., 2014; Norcia et al., 2015; Vialatte et al., 2010; Wieser et al., 2016).

3-Analyzing frequency tagging data: a step-by-step demonstration

3.1-The example data sets

Example data from one adult (Silva et al., 2021) and one infant (Barry-Anwar et al., in preparation) are provided on the Open Science Framework companion site of this paper. Both data sets have undergone initial segmenting, filtering, and artifact control. The functions provided in the FreqTag toolbox expect a 3-dimensional MATLAB array with dimensions of sensors, time points, and trials, as produced by widely used preprocessing tools including EEGLAB (Delorme & Makeig, 2004), ERPLAB (Lopez-Calderon & Luck, 2014) as well as other preprocessing pipelines used for infant data including HAPPE (Gabard-Durnam et al., 2018); MADE (Debnath et al., 2020), PREP (Bigdely-Shamlo et al., 2015), and ADJUST (Leach et al., 2020) and readily exported from environments such as BrainVision Analyzer (BrainVision Analyzer, Brain Products GmbH, Gilching, Germany), fieldtrip (Oostenveld et al., 2011), MNEPython (Gramfort et al., 2013).

3.1.1- Adult data set

The first example data set data comes from a study with adult observers (Silva et al., 2021). The full data set for this study can be found at: https://osf.io/a53s9/?view_only=1966f70fac954bac886381f908c7a275. For the sample data provided here, EEG was recorded from 129 channel geodesic EEG recording net (Philips EGI, OR, USA) while faces and novel objects (Sheinbugs, see Jones et al., 2018) were concurrently presented, fully spatially overlapping with each other, and rapidly contrast-modulated. Two different temporal rates, 5 Hz and 6 Hz, one used for faces and one for objects (counterbalanced

183 across participants). The experimental design is depicted in Figure 1. Both stimuli periodically
184 emerged at their tagging frequency from a Brownian noise (spatial noise with a $1/f^2$ characteristic)
185 patch with the same mean luminance and contrast as the experimental stimuli for a duration of
186 6000 ms for 70 trials.

187 [Insert Figure 1 here]

188 3.1.2- Infant data set

189 The second example data set is taken from a recently completed infant investigation using
190 frequency tagging. The entire data set, and stimuli are available at: Barry-Anwar et al., in
191 preparation; OPEN NEURO- BIDS format. Parents of all participants gave informed consent prior
192 to testing. EEG data were collected using a 129-channel Electrical Geodesic system (Net Amps
193 400, Phillips EGI, Eugene, OR). A subset of 109 sensors were kept for analysis. Infants viewed up
194 to 20 6-second trials (sample data are from a 9-month-old). Frequency tagging parameters, stimuli,
195 and trial duration were the same as in the adult sample.

196

197 3.2 Using this document and planning the analyses

198 The following step-by-step instructions reflect operations that are part of prototypical
199 pipelines for visualizing and analyzing data from a frequency-tagging study. Readers are
200 encouraged to follow along with the example pipeline code supplied on the github companion site
201 in the matlab live script (.mlx) format (freqtag_pipeline_example1.mlx, and
202 freqtag_pipeline_example2.mlx), or the corresponding .m file scripts. Live scripts allow users to
203 read background documentation and execute the code stepwise, while examining inputs and
204 outputs along with visualizations of each step. Thus, these live scripts and their accompanying
205 documentation detail many technical aspects and usage of the functions employed in the pipeline.

206 The description of these steps in the present paper focuses on conceptual issues. It is thus not
207 sufficient as a user's manual for the toolbox.

208 Importantly, when planning an analysis pipeline, the use of the analyses described in this
209 report depends on 1) the duration of the stimulation epoch, or how many seconds the stimuli array
210 was presented, and 2) the number of trials (how many times the stimulus array was repeated) by
211 experimental condition (see Figure 2). As a rule of thumb, analyses of time-varying changes in
212 the envelope of the ssVEP at each tagging frequency require durations of several seconds and
213 numbers of trials per condition that are comparable with studies of late event-related potentials
214 such as the P3, which have commensurate signal-to-noise ratio. By contrast, if time information is
215 discarded, within-trial averaging across several seconds of ssVEP may be applied using sliding
216 window procedures, substantially boosting the signal-to-noise ratio and allowing spectral analyses
217 at the level of single trials in many cases (see Figure 2). The present report illustrates typical
218 pipelines applied at the single participant level and includes quality checks and suggestions for
219 establishing the robustness of the spectral estimates.

220 [Insert Figure 2 here]

221

222 3.3-Example 1: Determining the ssVEP spectrum and measuring the envelope time course

223 In this first example, we describe a pipeline for quantifying the ssVEP in the frequency and
224 time-frequency domains, applicable for studies in which substantial numbers of trials are available
225 for averaging. The pipeline "freqtag_pipeline_example1.mlx" involves planning considerations,
226 and the usage of three toolbox functions, freqtag_FFT, freqtag_FFT3D, and freqtag_HILB.

227

3.3.1 Assessing data quality and preparing a barebones spectral analysis

The first step towards quantifying the ssVEP amplitude for the tagging frequencies is the computation of the amplitude spectrum using the Discrete Fourier Transform (DFT). This transform produces an amplitude spectrum, in which frequency is shown on the x-axis and amplitude at each frequency is plotted on the y-axis. In a spectral analysis not all frequencies are available and their distribution along the x-axis is determined by the Fourier uncertainty principle (for detailed discussion see: Bach & Meigen, 1999; Keil, 2013). According to this principle, the frequency resolution is determined by the duration of the EEG data segment used for the frequency analysis. Specifically, the smallest possible step-width on the x-axis of a spectrum is given as the inverse of the duration of the data segment entering the analysis, in cycles per second, measured in Hertz (Hz). Thus, transforming a time segment of 2 seconds from the time into the frequency (spectral) domain results in a spectrum with ½ = 0.5 Hz frequency resolution and a frequency axis, drawn on the x, which contains the frequency from 0 to half of the sampling rate in steps of .5 Hz. By the same token, transforming a time segment with a duration of 5 seconds will result in a spectrum spaced at ⅕ = 0.2 Hz.

After establishing these cornerstones of the planned analysis, we apply them to the example data files. The first dataset (exampledata_1.mat) was recorded with a sample rate of 500 Hz and has already been filtered by means of a 30-Hz low-pass (18th order Butterworth) and a 1-Hz high-pass (4th order Butterworth). The epochs were extracted from continuous EEG data, containing 400ms pre- and 7400ms post-stimulus onset (see Silva et al., 2021 for detailed description). Thus, if researchers were to transform the entire segment, including the pre-stimulus data, into the frequency domain, the frequency resolution would be 0.1282 (frequency resolution = 1/7.802, i.e., one divided by the segment's duration in seconds). However, in studies with frequency tagging it

is likely that researchers are interested in determining the spectrum selectively for the period of time during which ssVEP stimulation was present. In addition, it is often preferred to exclude the early portion of the stimulation epoch. This practice eliminates confounds of the ssVEP signal with potential transient ERPs evoked by the onset of the frequency tagging array and assists in focusing the analysis on the segment during which the ssVEP has reached a steady, stationary state.

In the example adult data, we select a segment starting 1 second after the onset of the frequency tagging array and ending at 7 seconds after the onset of the Brownian noise. In the pipeline this segment is called "data_ssvep". Considering the Nyquist Theorem and the sampling rate (500 Hz), we know that the highest frequency to be analyzed for the dataset is 250 Hz. Therefore, between 0 Hz and 250 Hz, in steps of 0.2 Hz (1/5 seconds), the spectrum contains 1251 frequencies.

$$\text{Highest (Nyquist) Frequency} = \frac{Sampling\ Rate}{2};$$

$$\text{Frequency Resolution} = \frac{1}{Epoch\ Duration\ in\ secs};$$

To implement ssVEP frequency-tagging in this task, Silva and colleagues (2021) used two different rates, 5 Hz and 6 Hz, one used for faces and one for objects. An initial manipulation check includes making sure that the dataset's frequency resolution can discriminate between the frequencies used for tagging and that the x-axis of the spectrum contains a bin at the exact stimulation frequencies. It is common practice to remove frequencies unrelated to the focus of your analysis and frequencies that are not related to brain activity. In this case, the frequencies kept for further analysis are those between 0 and 32.33Hz, called *faxis* in freqtag_pipeline_example1.mlx.

In general, it is good practice to visualize the data after each step of the analysis. Using the plot command, readers can plot the data in the time domain as an event-related potential (see Figure 3). In Figure 3, the x-axis represents time, and the y-axis represents the amplitude. Examples for plotting the data are provided throughout the freqtag_pipeline_example1.m script.

[Insert Figure 3 here]

3.3.2 – Conducting a barebones Fourier Transform: the freqtag_FFT function

The Fourier Theorem states that any given time domain signal can be represented in the frequency domain by a sum of sine and cosine waves with different frequencies, amplitudes, and phases. Several excellent tutorials on the foundations of Fourier analysis in EEG research are available for readers interested in learning more about its mathematical principles (Cohen, 2011; Keil, 2013). Many implementations of spectral analyses for EEG data exist, most of which involve application of so-called taper windows, within-segment averaging, zero-padding, or differential weighting of time points entering spectral analysis. However, for ssVEP analyses, a Fourier transform with no or minimal modifications (i.e., a barebones implementation) may yield the most unbiased estimate of ssVEP amplitude and phase (for a discussion, see Bach & Meigen, 1999).

At this stage of the pipeline, researchers make a key conceptual decision regarding the nature of the ssVEP signal: Traditionally, the ssVEP has been regarded an “evoked” response, which means that it is defined by being exactly time and phase-locked to the tagging stimulus, and thus analyzed analogous to event-related potentials. Specifically, a sufficient number of trials, with the same driving stimulus array, are collected and averaged in the time domain to suppress activity that is not locked to the timing of the periodically modulated stimulus. In the present case, this is

accomplished by averaging across the third dimension of the data array (trials). The resulting 2-dimensional time-domain average (sensors by time points) is then submitted to a spectral analysis. This is accomplished by the function freqtag_FFT.m, which uses the MATLAB built-in Discrete Fourier Transform algorithm (FFT.mat) without windowing or padding. This function outputs the amplitude spectrum, the phase spectrum, the complex spectrum of Fourier components, and a vector (list) of the frequency bins available in the spectrum.

3.3.3 – Conducting a Fourier Transform on single trials: the freqtag_FFT3D function

A second approach to conceptualizing the ssVEP is to emphasize the flexible entrainment of ongoing brain oscillations by the driving stimulus array. Under this assumption, not all of the ssVEP signal is exactly time- and phase-locked across trials and trial averaging may thus cause information loss (Gulbinaite et al., 2019). Researchers adopting this view have often analyzed the ssVEP by transforming each individual trial into the spectral domain followed by averaging the resulting single-trial amplitude spectra, thus avoiding cancellation of activity at the driving frequency that is not exactly time-locked across trials. In the present pipeline, this is accomplished by the function freqtag_FFT3D.m, which uses the initial 3-D data array (data_ssvep) containing electrodes, time points, and trials (for the third dimension). This function applies the Fourier Transform on each trial and averages the resulting spectra.

This latter approach is suggested for researchers who are interested in quantifying ssVEP activity while assuming that the phase may vary from trial to trial. For more experienced users, freqtag_FFT3D also outputs the complex spectrum for each trial, which can be used to calculate measures of variability and consistency of the ssVEP response, such as the circular T^2 statistic proposed by Victor and Mast (1991), or the Rayleigh statistic. The present paper cannot provide an in-depth discussion of these metrics, but readers are encouraged to consider metrics based on

complex representations, including when planning a study, as discussed in Baker et al. (2021). The toolbox also includes a version of the circular T^2 statistic, for application with the output of freqtag_FTT3D, or freqtag_slidewin, discussed below.

The typical way of illustrating the results of the Fourier Transform is a 2-D plot with frequency on the x-axis and amplitude on the y-axis. For visualization purposes, readers may wish to select a subset of the available frequencies. In the present example, both the evoked spectrum (after averaging in the time domain; Figure 4 – top panel) and the single-trial based spectrum (averaging the single trial spectra; Figure 4 – bottom panel) show not only the activity at the stimulus tagging frequency (5 Hz and 6 Hz peaks) but also at other frequencies. These frequencies include multiples of each tagging frequency (harmonics, e.g., at 10 and 12 Hz) but also some linear combinations of the two driving frequencies (intermodulation frequencies, e.g., at 4 Hz). There is a growing literature on how these additional responses may be used to test hypotheses regarding neural function (Appelbaum et al., 2006; Kim et al., 2005; Kim & Verghese, 2012). In a typical application, the amplitude at occipital sensors will serve as the dependent variable for statistical analysis, potentially after being converted to a signal-to-noise ratio (see 3.4.3 for an implementation of this step).

[Insert Figure 4 here]

3.3.4 – Using the Hilbert Transform to extract time-varying ssVEP amplitude envelopes: the freqtag_HILB function

Research questions addressed in frequency tagging studies often involve the time course of visuocortical activity assessed separately for stimuli in the tagging array. One method for extracting the time course of a narrow-band oscillatory waveform is the Filter-Hilbert method.

This method involves the Hilbert transform, a mathematical approach to generate a 90° phase-shifted version of the empirical time series, which then directly translates into a time-varying envelope measure. A core requirement for accurately determining and shifting the phase of the empirical signal is that the data used to perform the Hilbert transform are narrowly bandpass filtered. Although the Hilbert method can be readily applied to broadband signals containing activity at multiple frequencies, its results will range from difficult to interpret to meaningless because it uses phase-shifting, and the phase of a signal is only defined for a specific frequency.

Given the importance of digital bandpass filtering in the context of the Hilbert transform, readers may wish to peruse suitable tutorials and reviews of digital filtering as used in human electrophysiology (Luck, 2005; Nitschke et al., 1998; Rousselet, 2012; Widmann et al., 2015). The present paper uses simple and straightforward Butterworth filters. In brief, bandpass filtering is achieved by the construction of a kernel that is convolved with the EEG data to both preserve the frequencies of interest and attenuate the undesired frequencies. To create such kernel, it is necessary to define the filter shape and the frequency characteristics that define that shape. Designing a Butterworth filter in Matlab involves two input arguments: the filter order and the cutoff frequency. The filter order determines the precision of the filter's frequency response. Sharper roll-offs produced by higher filter order may increase the edge artifact expected to arise from filtering segmented data, and they heighten the delay of the filter onset response. Therefore, readers should carefully select the filter and visualize the data in order to control these artifacts. Once the kernels are built, the data can be filtered by means of the "filtfilt" function which is a zero-phased forward and reverse digital infinite-impulse filtering procedure. The function freqtag_HILB contains all of these steps such that the filtered version of the data is computed within the function and passed into the built-in MATLAB function "Hilbert".

The results of the Hilbert Transform are the outputs "hilbamp," "phase," and "complex." The variables "hilbamp" and "phase" contain the information of how amplitude and phase of the tagging frequency change over time. The variable "complex" contains both the empirical (real part) and phase-shifted (imaginary part) of the ssVEP, combined into one complex number for each time point. To visualize how the ssVEP amplitude at the frequency of interest changes over time, readers may plot the time-varying amplitude ("hilbamp"; see Figure 5).

[Insert Figure 5 here]

3.4 – Example 2. Using the sliding window approach to estimate the ssVEP in single trials

Not all research questions are readily addressed using information that is pooled across trials. Experimenters may wish to quantify the trial-by-trial change of visuocortical processing across only one experimental session or may wish to apply trial-based modeling of learning, habituation, adaptation, or other concepts that are at odds with trial averaging. Furthermore, limitations specific to the design or the population may prevent researchers from obtaining enough trials to enable the approach discussed in 3.3 above. Figure 6 represents the amplitude spectra obtained after the Fourier Transform, the expected driving frequencies and harmonic peaks are not as clear as the adult amplitude spectra shown in Figure 4. In many of these cases, it is possible to quantify the ssVEP amplitude evoked by a specific tagging stimulus at the level of single trials, using a simple sliding window method (Morgan et al., 1996; Wieser et al., 2016). Here, we use an example data set obtained from infants to illustrate this method, which may be particularly helpful

388 in developmental studies with few available trials. The procedures are illustrated in the
389 accompanying live script freqtag_pipeline_example2.mlx.

390 [Insert Figure 6 here]

391 3.4.1. Implementing the sliding window analysis: the freqtag_slidewin function

392 Sliding window analyses capitalize on the regularity of the driving stimulus and its evoked
393 brain electric response, at a known frequency. The rationale is simple: given sufficient trial
394 durations, a sliding average window that contains a suitable number of integer cycles of the driving
395 frequency (in our example, 4 cycles) can be shifted across the ssVEP segment of interest, in steps
396 that correspond to a full cycle of the oscillation (e.g., Morgan et al., 1996). Continuous averaging
397 of the contents of these sliding windows amplifies any oscillation that is time and phase-locked to
398 the driving stimulus and attenuates oscillations that vary in terms of their phase or frequency.

399 The example infant data set (exempledata_2.mat) has a 3-dimensional MATLAB array
400 with channels (109), time points (2500), and trials (after artifact detection 15 out of 20). During
401 preprocessing and segmenting, the time points that were not of interest have been removed and the
402 remaining 2500 sample points represent the duration of the frequency tagging array containing
403 faces and objects, tagged at 5 and 6 Hz. To implement the sliding window analysis, we use the
404 function freqtag_slidewin.m, which executes all steps needed for this analysis, including the
405 sliding window averaging and subsequent spectral analysis. This function applies a sliding window
406 analysis as described in Wieser et al., 2016 to each trial, at a given frequency.

407 The freqtag_slidewin function requires as input arguments: the data in a 3-D format
408 (sensor-by-time points-by-trials), a flag to determine whether or not to plot the sliding window
409 process (plotfag), a vector containing the sample points to be used for baseline subtraction (bslvec),

410 a vector containing the sample points to be used in the sliding window procedure (ssvepvc), the
411 driving frequency (foi = 5 or 6), a new sample rate if needed (fsampnew, see below), the sampling
412 rate (fsamp = 500Hz), and an out name. The baseline correction is necessary to remove drift, which
413 may induce spectral leaking. In the present example, exampledata_2 only contains the data
414 segment during which the stimuli were flickering. If users are working with epochs containing
415 other stimuli, they may assign only the time window of interest using the ssvepvec argument.
416 The function computes the duration, the onset times, and the number of sliding windows.
417 These windows contain 4 cycles of the driving frequency of interest and are stepped across the
418 ssVEP segment in steps of one cycle. For example, when extracting the 5 Hz ssVEP, the sliding
419 window contains 4 cycles of 200 ms (the wavelength at 5 Hz), thus being 800 ms long. Second,
420 the window is then moved across the EEG segment of interest in each trial, in steps of 200 ms,
421 corresponding to one full cycle of the driving frequency at 5 Hz.
422 At a driving rate of 6 Hz, the corresponding window length is 666.667 ms, to be moved
423 over the EEG segment in steps of 166.667 ms. Thus, at a sampling rate of 500 Hz, there will be no
424 integer numbers of sample points that accommodates the step-width or window length. As
425 explained above (section 2.2), this will lead to spectral leaking due to including incomplete cycles
426 entering the analysis. It is thus necessary to upsample the data to a rate that allows representation
427 of integer cycles of the driving frequency. As discussed in Bach & Meigen, 1999, an integer
428 relation between monitor retrace and sample rate is required to ensure the capture of each available
429 driving frequency by an integer number of sample points. In our example, this can be accomplished
430 by upsampling the data to 600 Hz, implemented by setting the “sampnew” input argument
431 accordingly. Setting the plotting flag to 1 produces a time-varying representation of each new

sliding window and the running average. Default outputs of the function are the trial-by-trial spectral amplitude at the frequency of interest, at each electrode (trialamp), and a 3-dimensional array that contains the sliding average in the time domain, for each trial and sensor (winmat).

One potential concern when using short segments of data is the cross-contamination of one tagging frequency by the other frequency, which is present in the signal, but not centered at another frequency bin. This concern may be particularly relevant when tagging frequencies occupy nearby spectral bins, as is the case in the example data sets used here: When applying the sliding window method to extract 6 Hz ssVEP responses from single trials, there is no bin at 5 Hz in the spectrum used to measure the 6 Hz response, which has bins at steps of 1/0.666 = 1.5 Hz. In most practical situations, the sliding window average technique however suppresses responses outside the target frequency. To illustrate this, the toolbox contains a simulation (simulsidebands.m) of how varying the amplitude of one tagging frequency affects the ssVEP amplitude measurement at the other (target) frequency and vice versa, when using the sliding window approach. Across a range of signal and noise levels, this simulation (See Appendix C and accompanying code) shows that, given typical trial lengths and stimulation rates, cross-talk between tags does not significantly affect amplitude estimation with the sliding window average method. As is also shown in appendix C, crosstalk does affect certain measures of signal-to-noise ratio, especially in cases where the tags are nearby and when the signal-to-noise ratio of the frequency of interest is low. Thus, users are

encouraged to use caution when using signal-to-noise ratios in combination with the sliding window method.

3.4.2. Computing variables of interest: amplitude and phase-stability

The default outputs of the sliding window function may not always be suitable for testing the hypothesis of interest in a given study. For example, if researchers are not interested in the trial-wise variation of the ssVEP they may wish to combine spectral information across trials, or to calculate amplitude after pooling the time-domain sliding window averages for each trial. For example, in studies with few trials in which the analyses described in 3.3 are unavailable. Like the rationale explained in 3.3 for time-domain averaging prior to spectral analysis, researchers may combine the single trial averaged windows into a cross-trial average, emphasizing the portion of the oscillation that is time and phase locked to the driving stimulus across repeated trials.

This can be accomplished by averaging the time-domain information contained in the winmat (winmat3d5Hz or winmat3d6Hz) in the third dimension (trials). The new time series (meanwinmat, electrode-by-time-points) can, then, be used as the input argument for the freqtag_FFT function. The frequency spectrum of the sliding windows can be plotted using the *bar* built-in MATLAB function (Figure 7, left panel), where the y-axis is the amplitude at each time-point (variable “amp”) and the x-axis is the frequency axis (variable “freq”). Alternatively, the spectral amplitude extracted from each trial may be averaged across trials, allowing

contributions to the trial averaged amplitude independent of the within-trial phase, using the function freqtag_FFT3D.

[Insert Figure 7 here]

As discussed in Wieser et al., 2016 researchers may also wish to test hypotheses regarding the stability of the tagged oscillation within each trial, measured as the phase similarity between all of the sliding windows. If the phase or latency of the ssVEP changes within a trial, relative to the periodic driving stimulus, then the phase similarity will be lower. If the phase relationship between the ssVEP and the driving stimulus remains stable across the duration of the trial, then the phase at the driving frequency should be similar across all sliding windows. Phase similarity is readily quantified using the phase-locking index, in which normalized complex phase values (real and imaginary part of the Fourier transform) are averaged and the absolute value (vector length or the Euclidean norm) of the average is the phase similarity index. The freqtag_slidewin function computes the phase stability index for each trial and outputs a value for each electrodes and trial as 2-dimensional matrix (electrodes by trials), which can then be statistically analyzed and plotted using EEGLAB/ERPLAB.

3.4.3 – Computing the signal-to-noise ratio: freqtag_simpleSNR

Finally, as was visible from the amplitude spectra shown in 3.3.2 (see Figure 4), spectral peaks located at the ssVEP amplitude often sit on top of other spectral phenomena which may include ongoing oscillatory activity or non-periodic activity. Thus, a comparison of raw amplitude often is difficult, as the amplitude estimate may confound ssVEP with non-ssVEP amplitude at the frequency of interest. Researchers have addressed this problem by computing signal-to-noise ratios

or similar measures (e.g., baseline corrected amplitude) for determining the distance between the ssVEP amplitude peak of interest from spectral noise in the same region of the spectrum (see e.g. Rossion et al., 2012). This issue has also been discussed for non-ssVEP spectral signals, which are often difficult to distinguish from non-periodic activity: Several advanced methods have been developed to separate oscillatory activity from other contributions to the spectrum (Donoghue et al., 2020). These methods often rely on estimating the overall shape of the amplitude spectrum which tends to take the shape of an exponential (1/f) function.

In the case of ssVEP spectra after trial averaging however, or with shorter segments as used in sliding window analyses, the spectrum tends to be overall flat, with the ssVEP tagging frequency visible as a signal. In the present report, we provide a widely used and simple approach for addressing this issue and measure the ratio of the amplitude at a given driving frequency over the mean amplitude measured at suitable neighboring (non-ssVEP) frequencies, by means of the freqtag_simpleSNR function.

As shown in the example, the selection of adjacent frequencies for the noise estimation aims to avoid other tagging frequencies, harmonics, and intermodulation frequencies (linear combinations of the tagging frequencies). The resulting ratios can be exported for hypothesis testing as unitless ratios, but also converted into decibels. One way to plot the result as decibels, using the *bar* built-in MATLAB function, is using the SNRdb output of this function (SNRdb5Hz or SNRdb6Hz) as the y-axis and the "freq" as the x-axis (Figure 8). "freq" is a variable originated through the freqtag_FFT and contains all the available frequencies as a vector.

To fully take advantage of the barebones functions provided in this toolbox, readers are invited to consult extant review papers on ssVEPs and the frequency tagging approach (Norcia et

al., 2015; Wieser et al., 2016). Furthermore, the functions provided here are readily combined with functions from other MATLAB-based analysis environments, which may add additional functionality. Finally, the code provided is intended to be tailored to specific research questions and populations. Many of the intermediate results computed in this pipeline may be used in ways that suit researchers interested in concepts like connectivity, neural competition, source distribution, and inter-trial variability of visuocortical signals (e.g., see Barry-Anwar et al., under review; Silva et al., 2021)

4- Summary and outlook

The goal of this article was to provide readers with conceptual and practical building blocks for ssVEP analysis for data collected using frequency tagging. The ability to individually quantify the individual visuocortical responses evoked by multiple concurrent and overlapping stimuli is a unique strength of this approach. Thus, frequency tagging allows testing hypotheses not typically addressable with other methods, including hypotheses regarding interactions between multiple items. Given its robust underlying signal, the method is highly suited for investigating populations that may be unable to sit through lengthy experimental sessions including infants, young children, and clinical populations.

5 -Acknowledgements

Funding for this work was provided L.Scott and A. Keil from by the National Science Foundation (BCS: #1728133) and the National Institute of Human Health and Child Development (R21HD102715-01). We thank members of UF's Center for the Study of Emotion and Attention, Martin Antov and Ryan Mears for bug reports and debugging assistance, the Brain, Cognition and

534 Development Laboratory and R. Barry-Anwar, Gabriella Silva, and Zoe Pestana for relevant
535 discussion, research assistance and technical and programming assistance.
536
537

6 -References

Ales, J. M., & Norcia, A. M. (2009). Assessing direction-specific adaptation using the steady-state visual evoked potential: Results from EEG source imaging. *Journal of Vision*, *9*(7), 8–8. https://doi.org/10.1167/9.7.8

Andersen, S. K., & Müller, M. M. (2015). Driving steady-state visual evoked potentials at arbitrary frequencies using temporal interpolation of stimulus presentation. *BMC Neuroscience*, *16*(1), 95. https://doi.org/10.1186/s12868-015-0234-7

Appelbaum, L. G., Wade, A. R., Vildavski, V. Y., Pettet, M. W., & Norcia, A. M. (2006). Cue-Invariant Networks for Figure and Background Processing in Human Visual Cortex. *The Journal of Neuroscience*, *26*(45), 11695–11708. https://doi.org/10.1523/JNEUROSCI.2741-06.2006

Bach, M., & Meigen, T. (1992). Electrophysiological correlates of texture segregation in the human visual evoked potential. *Vision Research*, *32*(3), 417–424. https://doi.org/10.1016/0042-6989(92)90233-9

Bach, M., & Meigen, T. (1999). Do's and don'ts in Fourier analysis of steady-state potentials. *Documenta Ophthalmologica. Advances in Ophthalmology*, *99*(1), 69–82. https://doi.org/10.1023/a:1002648202420

Baker, D. H., Vilidaite, G., Lygo, F. A., Smith, A. K., Flack, T. R., Gouws, A. D., & Andrews, T. J. (2021). Power contours: Optimising sample size and precision in experimental psychology and human neuroscience. *Psychological Methods*, *26*(3), 295–314. https://doi.org/10.1037/met0000337

Baker, T. J., Norcia, A. M., & Rowan Candy, T. (2011). Orientation tuning in the visual cortex of 3-month-old human infants. *Vision Research*, *51*(5), 470–478. https://doi.org/10.1016/j.visres.2011.01.003

Barry-Anwar, R., Hadley, H., Conte, S., Keil, A., & Scott, L. S. (2018). The developmental time course and topographic distribution of individual-level monkey face discrimination in the infant brain. *Neuropsychologia*, *108*, 25–31. https://doi.org/10.1016/j.neuropsychologia.2017.11.019

Barry-Anwar, R., Kutlu, E., Keil, A., & Scott, L. S. (in preparation). *EEG Frequency Tagging of Superimposed Faces and Objects in Adults and Infants*.

Barry-Anwar, R., Riggins, T., & Scott, L. S. (2020). Electrophysiology in developmental populations: Key methods and findings. In *The Oxford Handbook of Developmental Cognitive Neuroscience*. https://doi.org/10.1093/oxfordhb/9780198827474.013.3

Bell, M. A., & Cuevas, K. (2012). Using EEG to Study Cognitive Development: Issues and Practices. *Journal of Cognition and Development : Official Journal of the Cognitive Development Society*, *13*(3), 281–294. https://doi.org/10.1080/15248372.2012.691143

Bigdely-Shamlo, N., Mullen, T., Kothe, C., Su, K.-M., & Robbins, K. A. (2015). The PREP pipeline: Standardized preprocessing for large-scale EEG analysis. *Frontiers in Neuroinformatics*, *9*. https://doi.org/10.3389/fninf.2015.00016

Bombeke, K., Duthoo, W., Mueller, S. C., Hopf, J.-M., & Boehler, C. N. (2016). Pupil size directly modulates the feedforward response in human primary visual cortex independently of attention. *NeuroImage*, *127*, 67–73. https://doi.org/10.1016/j.neuroimage.2015.11.072

582 Braddick, O. J., Atkinson, J., & Wattam-Bell, J. R. (1986). Development of the discrimination of
583 spatial phase in infancy. *Vision Research*, *26*(8), 1223–1239.
584 https://doi.org/10.1016/0042-6989(86)90103-3
585 Buiatti, M., Di Giorgio, E., Piazza, M., Polloni, C., Menna, G., Taddei, F., Baldo, E., &
586 Vallortigara, G. (2019). Cortical route for facelike pattern processing in human
587 newborns. *Proceedings of the National Academy of Sciences of the United States of*
588 *America*, *116*(10), 4625–4630. https://doi.org/10.1073/pnas.1812419116
589 Christodoulou, J., Leland, D. S., & Moore, D. S. (2018). Overt and covert attention in infants
590 revealed using steady-state visually evoked potentials. *Developmental Psychology*, *54*(5),
591 803–815. https://doi.org/10.1037/dev0000486
592 Cohen, M. (2011). *Analyzing Neural Time Series Data: Theory and Practice* (p. 578). The MIT
593 Press.
594 de Heering, A., & Rossion, B. (2015). Rapid categorization of natural face images in the infant
595 right hemisphere. *ELife*, *4*, 1–14. https://doi.org/10.7554/eLife.06564
596 Debnath, R., Buzzell, G. A., Morales, S., Bowers, M. E., Leach, S. C., & Fox, N. A. (2020). The
597 Maryland analysis of developmental EEG (MADE) pipeline. *Psychophysiology*, *57*(6),
598 e13580. https://doi.org/10.1111/psyp.13580
599 Delorme, A., & Makeig, S. (2004). EEGLAB: An open source toolbox for analysis of single-trial
600 EEG dynamics including independent component analysis. *Journal of Neuroscience*
601 *Methods*, *134*(1), 9–21. https://doi.org/10.1016/j.jneumeth.2003.10.009
602 Di Russo, F., Pitzalis, S., Aprile, T., Spitoni, G., Patria, F., Stella, A., Spinelli, D., & Hillyard, S.
603 A. (2006). Spatiotemporal analysis of the cortical sources of the steady-state visual

evoked potential. *Human Brain Mapping*, *28*(4), 323–334. https://doi.org/10.1002/hbm.20276

Donoghue, T., Dominguez, J., & Voytek, B. (2020). Electrophysiological Frequency Band Ratio Measures Conflate Periodic and Aperiodic Neural Activity. *ENeuro*, *7*(6). https://doi.org/10.1523/ENEURO.0192-20.2020

Farzin, F., Hou, C., & Norcia, A. M. (2012). Piecing it together: Infants' neural responses to face and object structure. *Journal of Vision*, *12*(13), 1–14. https://doi.org/10.1167/12.13.6

Gabard-Durnam, L. J., Mendez Leal, A. S., Wilkinson, C. L., & Levin, A. R. (2018). The Harvard Automated Processing Pipeline for Electroencephalography (HAPPE): Standardized Processing Software for Developmental and High-Artifact Data. *Frontiers in Neuroscience*, *12*. https://doi.org/10.3389/fnins.2018.00097

Giabbiconi, C.-M., Jurilj, V., Gruber, T., & Vocks, S. (2016). Steady-state visually evoked potential correlates of human body perception. *Experimental Brain Research*, *234*(11), 3133–3143. https://doi.org/10.1007/s00221-016-4711-8

Gilmore, R. O., Hou, C., Pettet, M. W., & Norcia, A. M. (2007). Development of cortical responses to optic flow. *Visual Neuroscience*, *24*(6), 845–856. https://doi.org/10.1017/S0952523807070769

Gramfort, A., Luessi, M., Larson, E., Engemann, D. A., Strohmeier, D., Brodbeck, C., Goj, R., Jas, M., Brooks, T., Parkkonen, L., & Hämäläinen, M. (2013). MEG and EEG data analysis with MNE-Python. *Frontiers in Neuroscience*, *7*. https://doi.org/10.3389/fnins.2013.00267

Gulbinaite, R., Roozendaal, D. H. M., & VanRullen, R. (2019). Attention differentially modulates the amplitude of resonance frequencies in the visual cortex. *NeuroImage*, *203*, 116146. https://doi.org/10.1016/j.neuroimage.2019.116146

Hamer, R. D., & Norcia, A. M. (1994). The development of motion sensitivity during the first year of life. *Vision Research*, *34*(18), 2387–2402. https://doi.org/10.1016/0042-6989(94)90283-6

Handy, T. C. (Ed.). (2004). *Event-related potentials: A methods handbook*. Cambridge, MA: Bradford Books.

Jackson, A. F., & Bolger, D. J. (2014). The neurophysiological bases of EEG and EEG measurement: A review for the rest of us. *Psychophysiology*, *51*(11), 1061–1071. https://doi.org/10.1111/psyp.12283

Jaganathan, V., Srihari Mukesh, T. M., & Ramasubba Reddy, M. (2005). Design and implementation of high performance visual stimulator for brain computer interfaces. *Annual International Conference of the IEEE Engineering in Medicine and Biology - Proceedings*, *7 VOLS*, 5381–5383. https://doi.org/10.1109/iembs.2005.1615698

Jones, T., Hadley, H., Cataldo, A. M., Arnold, E., Curran, T., Tanaka, J. W., & Scott, L. S. (2018). Neural and behavioral effects of subordinate-level training of novel objects across manipulations of color and spatial frequency. *European Journal of Neuroscience*, *52*(11), 4468–4479. https://doi.org/10.1111/ejn.13889

Keil, A. (2013). Electro- and Magneto-Encephalography in the Study of Emotion. *The Cambridge Handbook of Human Affective Neuroscience*, 107–132.

Keil, A., Debener, S., Gratton, G., Junghöfer, M., Kappenman, E. S., Luck, S. J., Luu, P., Miller, G. A., & Yee, C. M. (2014). Committee report: Publication guidelines and

recommendations for studies using electroencephalography and magnetoencephalography. *Psychophysiology*, *51*(1), 1–21. https://doi.org/10.1111/psyp.12147

Kim, D., Zemon, V., Saperstein, A., Butler, P. D., & Javitt, D. C. (2005). Dysfunction of early-stage visual processing in schizophrenia: Harmonic analysis. *Schizophrenia Research*, *76*(1), 55–65. https://doi.org/10.1016/j.schres.2004.10.011

Kim, Y.-J., Grabowecky, M., Paller, K. A., & Suzuki, S. (2011). Differential Roles of Frequency-following and Frequency-doubling Visual Responses Revealed by Evoked Neural Harmonics. *Journal of Cognitive Neuroscience*, *23*(8), 1875–1886. https://doi.org/10.1162/jocn.2010.21536

Kim, Y.-J., & Verghese, P. (2012). The Selectivity of Task-Dependent Attention Varies with Surrounding Context. *Journal of Neuroscience*, *32*(35), 12180–12191. https://doi.org/10.1523/JNEUROSCI.5992-11.2012

Köster, M., Langeloh, M., & Hoehl, S. (2019). Visually Entrained Theta Oscillations Increase for Unexpected Events in the Infant Brain. *Psychological Science*, *30*(11), 1656–1663. https://doi.org/10.1177/0956797619876260

Leach, S. C., Morales, S., Bowers, M. E., Buzzell, G. A., Debnath, R., Beall, D., & Fox, N. A. (2020). Adjusting ADJUST: Optimizing the ADJUST algorithm for pediatric data using geodesic nets. *Psychophysiology*, *57*(8), e13566. https://doi.org/10.1111/psyp.13566

Leleu, V., Douilliez, C., & Rusinek, S. (2014). Difficulty in disengaging attention from threatening facial expressions in anxiety: A new approach in terms of benefits. *Journal of Behavior Therapy and Experimental Psychiatry*, *45*(1), 203–207. https://doi.org/10.1016/j.jbtep.2013.10.007

Lochy, A., de Heering, A., & Rossion, B. (2019). The non-linear development of the right hemispheric specialization for human face perception. *Neuropsychologia*, *126*, 10–19. https://doi.org/10.1016/j.neuropsychologia.2017.06.029

Lopez-Calderon, J., & Luck, S. J. (2014). ERPLAB: An open-source toolbox for the analysis of event-related potentials. *Frontiers in Human Neuroscience*, *8*. https://doi.org/10.3389/fnhum.2014.00213

Luck, S. J. (2005). *An Introduction to the Event-Related Potential Technique*. The MIT Press.

Luck, S. J & Kappenman, E. S (Eds.). (2013). *The oxford handbook of event-related potential components.* Oxford University Press.

Miskovic, V., & Keil, A. (2013). Perceiving Threat In the Face of Safety: Excitation and Inhibition of Conditioned Fear in Human Visual Cortex. *Journal of Neuroscience*, *33*(1), 72–78. https://doi.org/10.1523/JNEUROSCI.3692-12.2013

Morgan, S. T., Hansen, J. C., & Hillyard, S. A. (1996). Selective attention to stimulus location modulates the steady-state visual evoked potential. *Proc Natl Acad Sci U S A*, *93*(10), 4770–4774.

Mouraux, A., & Iannetti, G. D. (2008). Across-trial averaging of event-related EEG responses and beyond. *Magnetic Resonance Imaging*, *26*(7), 1041–1054. https://doi.org/10.1016/j.mri.2008.01.011

Muller, M. M., Andersen, S. K., & Keil, A. (2008). Time Course of Competition for Visual Processing Resources between Emotional Pictures and Foreground Task. *Cerebral Cortex*, *18*(8), 1892–1899. https://doi.org/10.1093/cercor/bhm215

693 Müller, M. M., Teder-Salejarvi, W., & Hillyard, S. A. (1998). The time course of cortical
694 facilitation during cued shifts of spatial attention. *Nat Neurosci*, *1*(7), 631–634.
695 Nitschke, J. B., Miller, G. A., & Cook, E. W. (1998). Digital filtering in EEG/ERP analysis:
696 Some technical and empirical comparisons. *Behavior Research Methods, Instruments,*
697 *and Computers*, *30*(1), 54–67. https://doi.org/10.3758/BF03209416
698 Norcia, A. M., Appelbaum, L. G., Ales, J. M., Cottereau, B. R., & Rossion, B. (2015). The
699 steady-state visual evoked potential in vision research: A review. *Journal of Vision*,
700 *15*(6), 4. https://doi.org/10.1167/15.6.4
701 Nunez, P. L., Nunez, E. P. of B. E. P. L., Srinivasan, R., & Srinivasan, A. P. of C. S. R. (2006).
702 *Electric Fields of the Brain: The Neurophysics of EEG*. Oxford University Press.
703 Odom, J., Bach, M., Barber, C., Brigell, M., Marmor, M., Tormene, A., Holder, G., & Vaegan.
704 (2004). Visual evoked potentials standard (2004). *Documenta Ophthalmologica.*
705 *Advances in Ophthalmology*, *108*, 115–123.
706 https://doi.org/10.1023/B:DOOP.0000036790.67234.22
707 Oostenveld, R., Fries, P., Maris, E., & Schoffelen, J.-M. (2011). FieldTrip: Open source software
708 for advanced analysis of MEG, EEG, and invasive electrophysiological data.
709 *Computational Intelligence and Neuroscience*, *2011*, 156869.
710 https://doi.org/10.1155/2011/156869
711 Park, J. (2018). A neural basis for the visual sense of number and its development: A steady-state
712 visual evoked potential study in children and adults. *Developmental Cognitive*
713 *Neuroscience*, *30*, 333–343. https://doi.org/10.1016/j.dcn.2017.02.011
714 Petro, N. M., Gruss, L. F., Yin, S., Huang, H., Miskovic, V., Ding, M., & Keil, A. (2017).
715 Multimodal Imaging Evidence for a Frontoparietal Modulation of Visual Cortex during

the Selective Processing of Conditioned Threat. *Journal of Cognitive Neuroscience*, *29*(6), 953–967. https://doi.org/10.1162/jocn_a_01114

Peykarjou, S., Hoehl, S., Pauen, S., & Rossion, B. (2017). Rapid Categorization of Human and Ape Faces in 9-Month-Old Infants Revealed by Fast Periodic Visual Stimulation. *Scientific Reports*, *7*(1), 1–12. https://doi.org/10.1038/s41598-017-12760-2

Regan, D. (1989). *Human brain electrophysiology: Evoked potentials and evoked magnetic fields in science and medicine*. Elsevier Science.

Riels, K., Campagnoli, R., Thigpen, N., & Keil, A. (2021). *Oscillatory brain activity links experience to expectancy during associative learning* [Preprint]. Neuroscience. https://doi.org/10.1101/2021.01.04.425296

Riggins, T., & Scott, L. S. (2020). P300 development from infancy to adolescence. *Psychophysiology*, *57*(7), e13346. https://doi.org/10.1111/psyp.13346

Robertson, S. S., Watamura, S. E., & Wilbourn, M. P. (2012). Attentional dynamics of infant visual foraging. *Proceedings of the National Academy of Sciences of the United States of America*, *109*(28), 11460–11464. https://doi.org/10.1073/pnas.1203482109

Rogala, J., Kublik, E., Krauz, R., & Wróbel, A. (2020). Resting-state EEG activity predicts frontoparietal network reconfiguration and improved attentional performance. *Scientific Reports*, *10*(1), 5064. https://doi.org/10.1038/s41598-020-61866-7

Rossion, B., Prieto, E. A., Boremanse, A., Kuefner, D., & Van Belle, G. (2012). A steady-state visual evoked potential approach to individual face perception: effect of inversion, contrast-reversal and temporal dynamics. *NeuroImage*, *63*(3), 1585–1600.

Rousselet, G. A. (2012). Does filtering preclude us from studying ERP time-courses? *Frontiers in Psychology*, *3*, 1–9. https://doi.org/10.3389/fpsyg.2012.00131

739 Silva, G., Rocha, H. A., Kutlu, E., Boylan, M. R., Scott, L. S., & Keil, A. (2021). Single-session
740 label training alters neural competition between objects and faces. *Journal of*
741 *Experimental Psychology: Human Perception and Performance*.
742 https://doi.org/10.1037/xhp0000889
743 Thigpen, N., Petro, N. M., Oschwald, J., Oberauer, K., & Keil, A. (2019). Selection of Visual
744 Objects in Perception and Working Memory One at a Time. *Psychological Science*,
745 *30*(9), 1259–1272. https://doi.org/10.1177/0956797619854067
746 Tononi, G., Srinivasan, R., Russell, D. P., & Edelman, G. M. (1998). Investigating neural
747 correlates of conscious perception by frequency-tagged neuromagnetic responses.
748 *Proceedings of the National Academy of Sciences*, *95*(6), 3198–3203.
749 https://doi.org/10.1073/pnas.95.6.3198
750 Vettori, S., Dzhelyova, M., Van der Donck, S., Jacques, C., Van Wesemael, T., Steyaert, J.,
751 Rossion, B., & Boets, B. (2020). Combined frequency-tagging EEG and eye tracking
752 reveal reduced social bias in boys with autism spectrum disorder. *Cortex*, *125*, 135–148.
753 https://doi.org/10.1016/j.cortex.2019.12.013
754 Vialatte, F.-B., Maurice, M., Dauwels, J., & Cichocki, A. (2010). Steady-state visually evoked
755 potentials: Focus on essential paradigms and future perspectives. *Progress in*
756 *Neurobiology*, *90*(4), 418–438. https://doi.org/10.1016/j.pneurobio.2009.11.005
757 Victor, J. D., & Mast, J. (1991). A new statistic for steady-state evoked potentials.
758 *Electroencephalogr Clin Neurophysiol*, *78*(5), 378–388.
759 Wang, J., Clementz, B. A., & Keil, A. (2007). The neural correlates of feature-based selective
760 attention when viewing spatially and temporally overlapping images. *Neuropsychologia*,
761 *45*(7), 1393–1399. https://doi.org/10.1016/j.neuropsychologia.2006.10.019

762 Wang, P., & Nikolic, D. (2011). An LCD Monitor with Sufficiently Precise Timing for Research
763 in Vision. *Frontiers in Human Neuroscience*, *5*.
764 https://doi.org/10.3389/fnhum.2011.00085
765 Widmann, A., Schröger, E., & Maess, B. (2015). Digital filter design for electrophysiological
766 data—A practical approach. *Journal of Neuroscience Methods*, *250*, 34–46.
767 https://doi.org/10.1016/j.jneumeth.2014.08.002
768 Wieser, M. J., & Keil, A. (2011). Temporal trade-off effects in sustained attention: Dynamics in
769 visual cortex predict the target detection performance during distraction. *Journal of*
770 *Neuroscience*, *31*(21), 7784–7790. https://doi.org/10.1523/JNEUROSCI.5632-10.2011
771 Wieser, M. J., McTeague, L. M., & Keil, A. (2011). Sustained preferential processing of social
772 threat cues: Bias without competition? *Journal of Cognitive Neuroscience*, *23*(8), 1973–
773 1986. https://doi.org/10.1162/jocn.2010.21566
774 Wieser, M. J., McTeague, L. M., & Keil, A. (2012). Competition effects of threatening faces in
775 social anxiety. *Emotion*, *12*(5), 1050. https://doi.org/10.1037/a0027069
776 Wieser, M. J., Miskovic, V., & Keil, A. (2016). Steady-state visual evoked potentials as a
777 research tool in social affective neuroscience. *Psychophysiology*, *53*(12), 1763–1775.
778 https://doi.org/10.1111/psyp.12768
779 Wieser, M. J., Reicherts, P., Juravle, G., & von Leupoldt, A. (2016). Attention mechanisms
780 during predictable and unpredictable threat—A steady-state visual evoked potential
781 approach. *NeuroImage*, *139*, 167–175. https://doi.org/10.1016/j.neuroimage.2016.06.026
782 Woodman, G. F. (2013). Viewing the dynamics and control of visual attention through the lens
783 of electrophysiology. *Vision Research*, *80*, 7–18.
784 https://doi.org/10.1016/j.visres.2013.01.003

785 Zhigalov, A., Herring, J. D., Herpers, J., Bergmann, T. O., & Jensen, O. (2019). Probing cortical
786 excitability using rapid frequency tagging. *NeuroImage*, *195*, 59–66.
787 https://doi.org/10.1016/j.neuroimage.2019.03.056

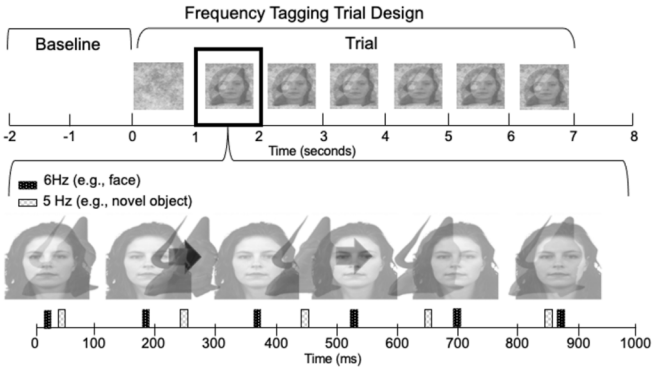

Figure 1: Experimental design modified from Silva et al., 2020. Segments used for Frequency and Time-Frequency analysis were 6 seconds long. The stimuli (faces and objects, flickering in 5hz and 6Hz) concurrently emerged from a Brownian noise background.

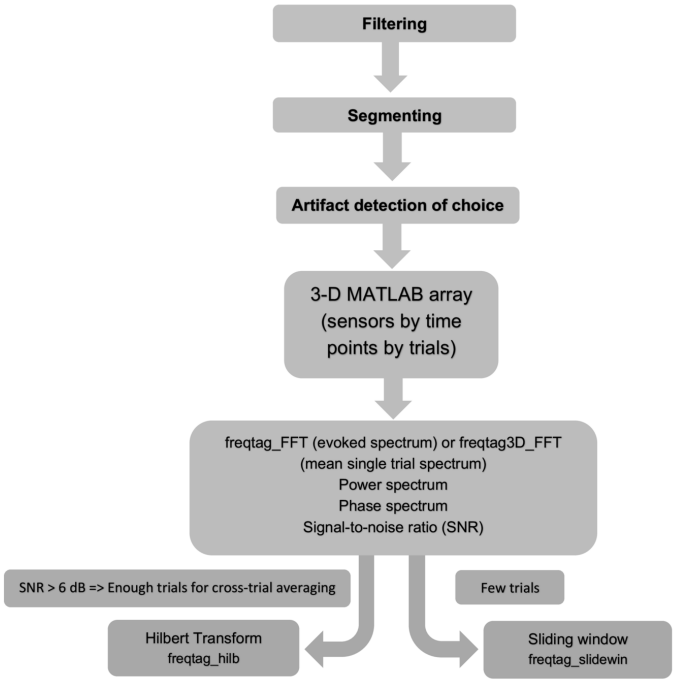

Figure 2: A decision tree for the choice of analysis purposes showing how the number of trials lead to two sets of different analyses.

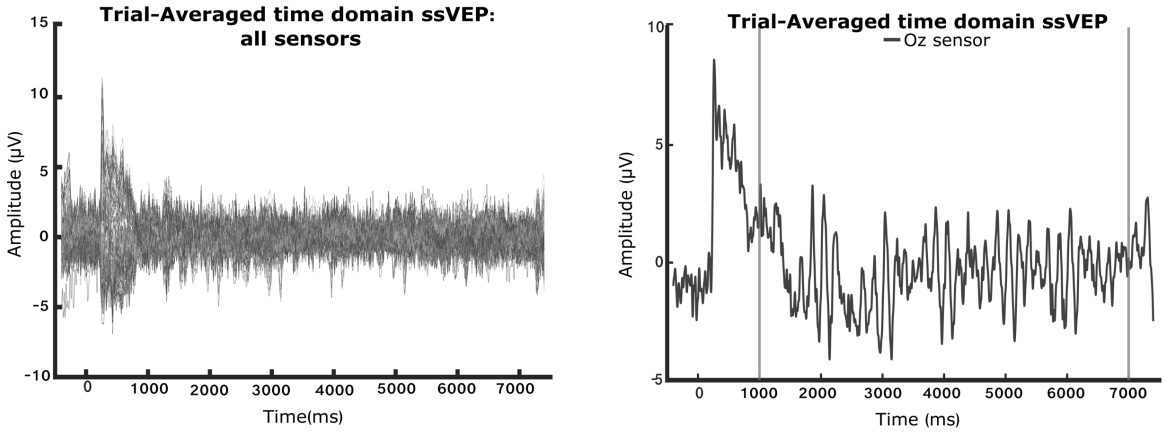

Figure 3: Adult dataset plotted in the time domain as an event-related potential by averaging the trials in the third dimension. On the left, all 129 sensors are plotted. On the right, only the Oz sensor is plotted. The two vertical bars indicate the 6-second analysis time-window.

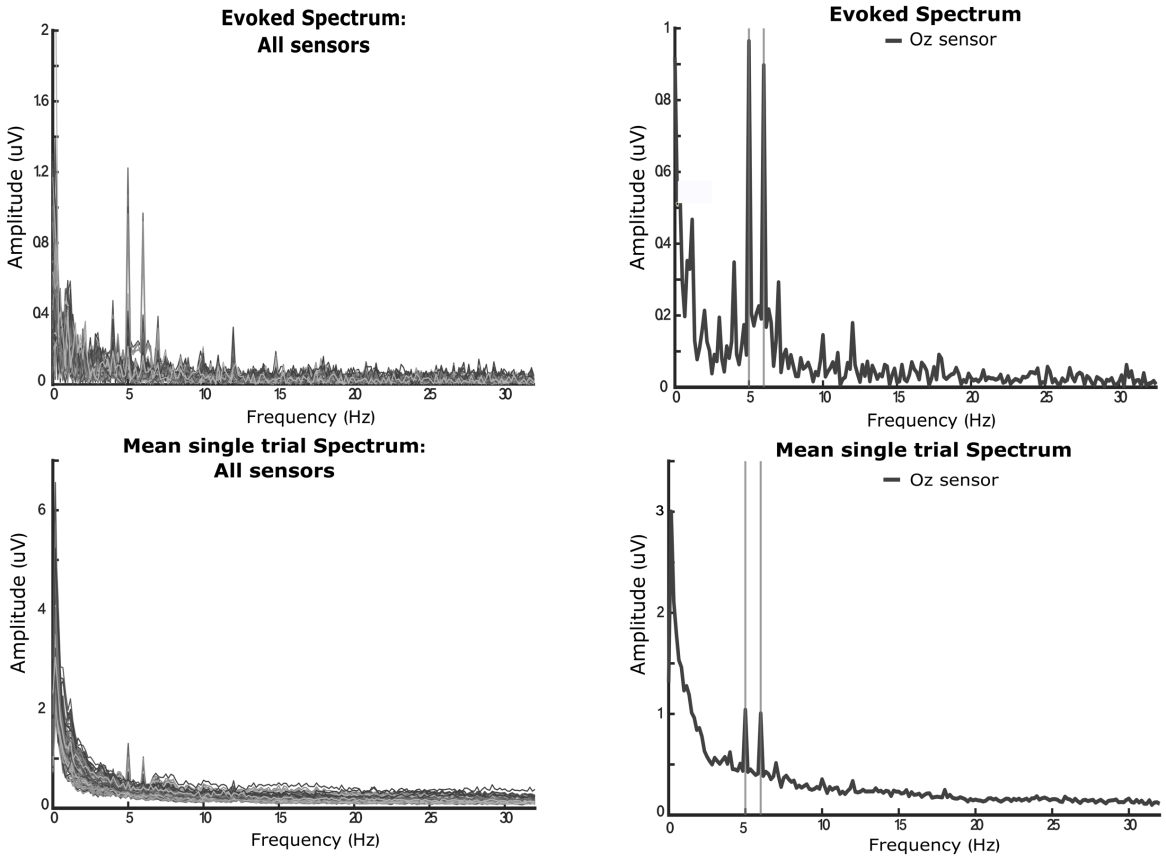

Figure 4: Two ways of applying the Fourier Transform: On the top panel, trials are averaged in the time domain followed by the execution of the freqtag_FFT.m function. In this case, the averaging procedure aims at suppressing the activity that is not time-locked to the driving frequency. On the bottom panel, a Fourier Transform is applied in each trial and the resulting spectra is averaged, this is accomplished by the freqtag3D_FFT.m. If the phase varies across trials, researchers can benefit from the later approach. Plots

on the left column contain the amplitude information for each frequency; each sensor is a line. Plots on the right column, contain the information from the Oz sensor.

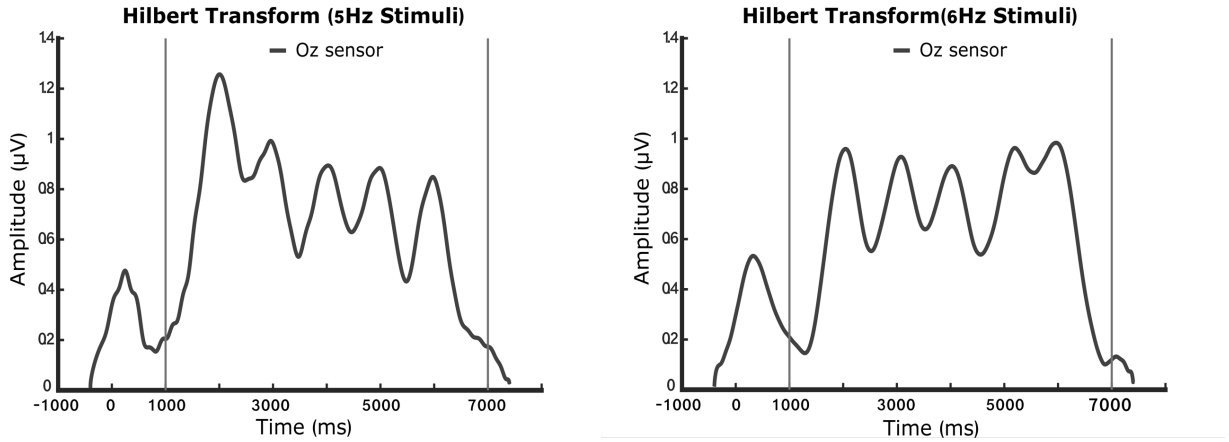

Figure 5: The time-varying ssVEP amplitude envelopes of the 5Hz (on the left) and 6Hz (on the left) tagging frequencies. This plot can be drawn using the results from the freqtag_HILB.m function.

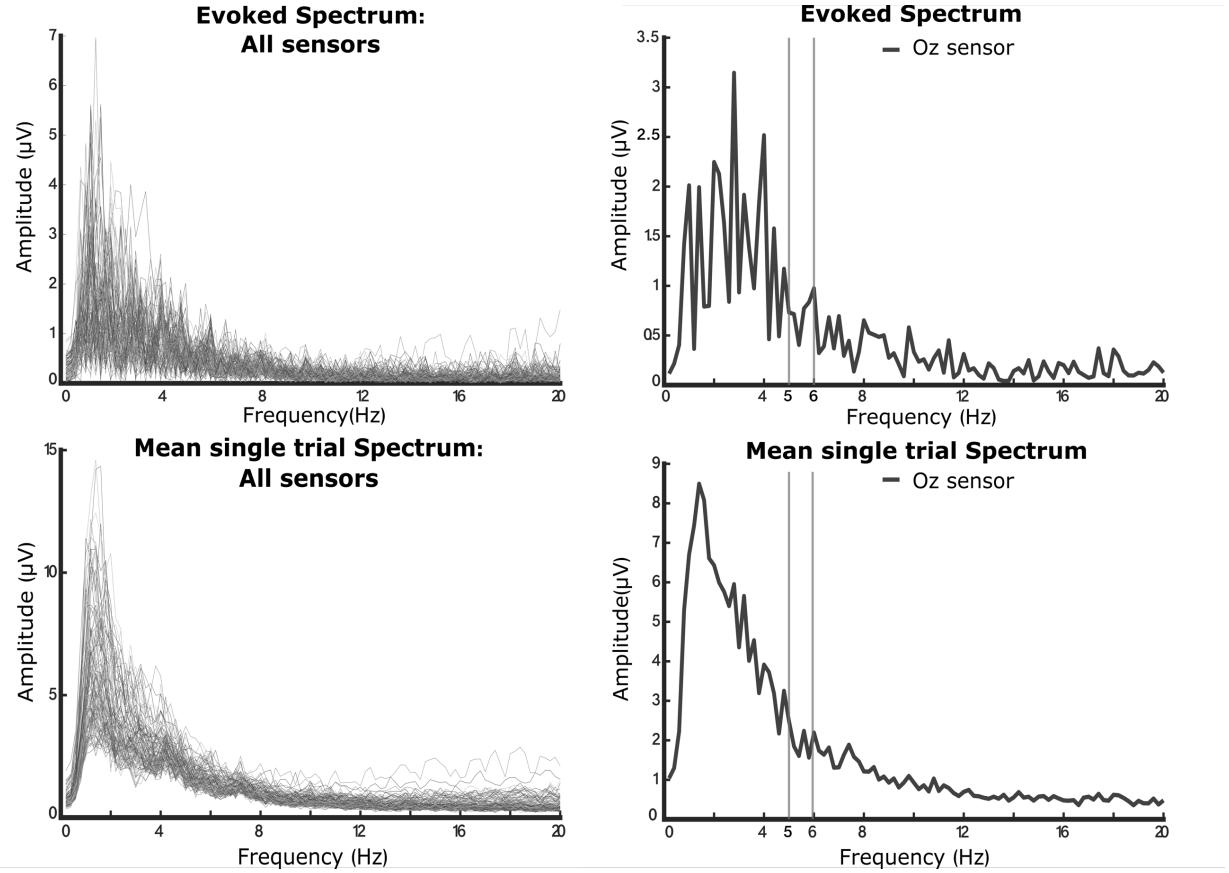

Figure 6: Amplitude spectra from the Fourier Transform applied to the infant data. The vertical bars indicate the tagging frequencies (5 and 6Hz). Although the spectra look as expected, it is not possible to obtain robust ssVEP response given the insufficient number of trials (less than 20). The evoked amplitude spectrum can be seen in the top panel, on the left, each electrode is a line and on the right the line represents the ssVEP amplitude at Oz. The mean amplitude of the single trial spectra is plotted on the bottom panel.

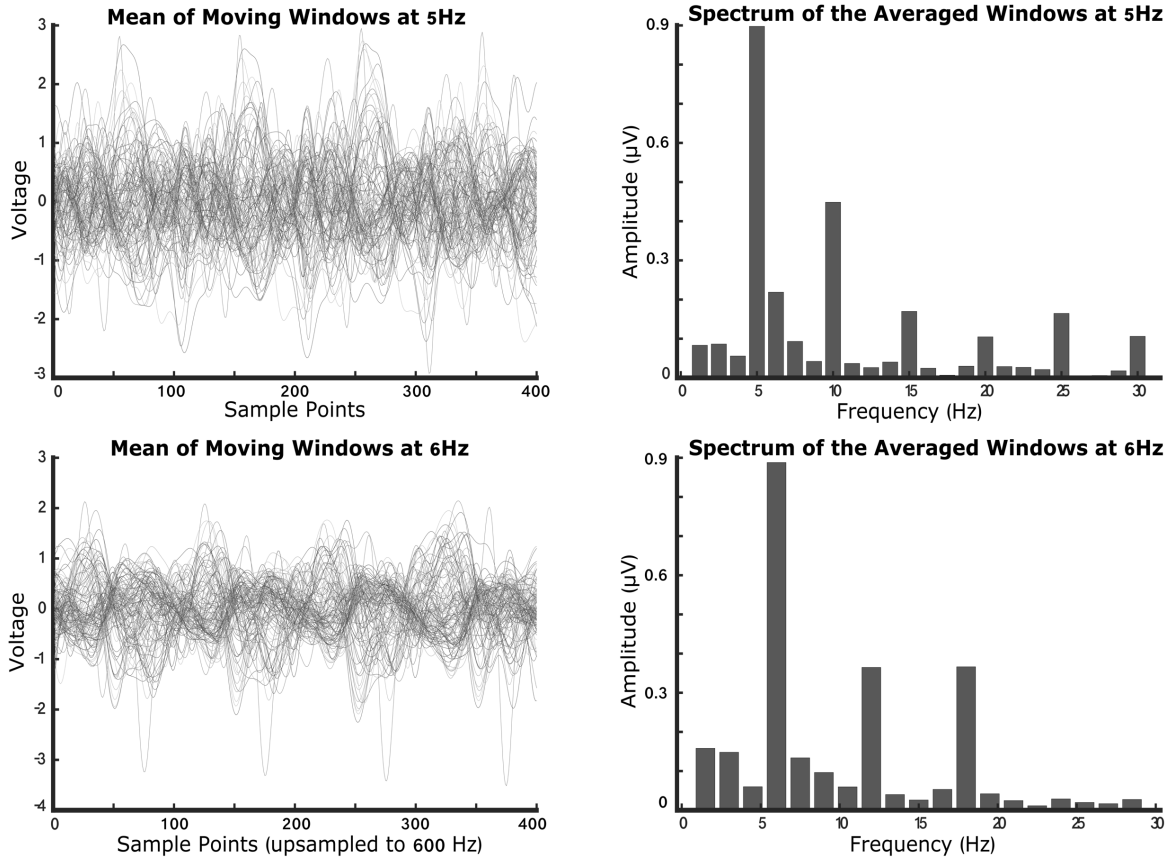

Figure 7: Moving window estimates. On the left panel, each line is a sensor that combines the single trials time-domain information of the evoked ssVEP at 5Hz (top) and 6Hz (bottom). The time series (meanwinmat) obtained from the freqtag_slidewin.m can be projected in the frequency domain by means of Fourier Transform (freqtag_FFT.m). The right panel shows the amplitude spectra of the sliding-window at 5Hz (top) and 6hz (bottom).